Quantum signatures of nonlinear resonances in mesoscopic systems: Efficient extension of localized wave functions

Y. F. Chen, T. H. Lu, K. W. Su, and K. F. Huang
Department of Electrophysics, National Chiao Tung University, Hsinchu, Taiwan
(Received 17 June 2005; revised manuscript received 12 August 2005; published 16 November 2005)

We investigate the quantum signatures of classical nonlinear resonances by making the analytic connection between the quantum wave functions and the classical periodic orbits for the uncoupled systems. It is found that the highly efficient extension of the localized coherent states within the classical caustics is an intriguing phenomenon in mesoscopic systems with nonlinear resonances. With the theoretical analysis, we experimentally demonstrate that the laser resonator with an intracavity saturable absorber can be employed to visualize the wave patterns analogous to the quantum wave functions associated with Fermi resonance.

DOI: 10.1103/PhysRevE.72.056210 PACS number(s): 05.45.Mt, 03.65.Ge, 45.05.+x, 42.60.Jf

I. INTRODUCTION

Investigations of the quantum ballistic transport in nanostructure devices have revealed that the intriguing observations of conductance fluctuations are closely related to the quantum wave functions associated with the classical periodic orbits [1–6]. In recent years, there has been growing attention to quantum manifestations of classical periodic orbits in mesoscopic systems [7–17]. Nonlinear resonances, which are originally described by Fermi in the molecule of CO_2 [18], have been shown to have a dramatic influence on the shapes of classical trajectories [19]. The phenomenon of nonlinear resonances play a crucial role in experimental studies of molecular excitations, tunneling effect, stellar trajectories, as well as other theoretical works [19–22]. Therefore, the connection between the quantum wave functions and the classical trajectories in mesoscopic systems with internal nonlinear resonances is important for understanding the quantum features of nonlinear classical dynamics, which is also a central issue in modern physics.

A single trajectory in the coupled Fermi resonance system often sweeps out a region similar to that described by an ensemble of periodic orbits in the uncoupled system [19]. Therefore, the wave functions related to classical periodic orbits in the zero-order systems can serve as an excellent basis to manifest the quantum effect of nonlinear resonances. In this paper, we analytically construct the connection between the quantum wave functions and the classical periodic orbits to investigate the quantum signatures of classical nonlinear resonances in mesoscopic systems. With the analytical formulism, we disclose that only a few localized stationary states in mesoscopic systems are already sufficient to extend wave patterns within the classical caustics to reveal the quantum features of nonlinear resonances. Moreover, we experimentally demonstrate that the quantum wave functions associated with 2:1 coupled resonance can be analogously visualized from the laser patterns emitted from a nearly hemispherical laser cavity with an intracavity saturable absorber.

II. CLASSICAL TRAJECTORIES IN THE 2D HARMONIC OSCILLATOR WITH NONLINEAR RESONANCE

A single classical trajectory in the coupled resonance system is usually found to cover a region similar to that of an ensemble of periodic orbits in the uncoupled system [19]. Here we present a brief synopsis for the purpose of completeness. Considering the 2D harmonic oscillator with nonlinear resonances, the Hamiltonian for this system can be generally modeled as

$$H = H_o + V_c, \tag{1}$$

where V_c is the coupling potential and

$$H_o = \frac{1}{2}(p_x^2 + p_y^2 + \omega_x^2 x^2 + \omega_y^2 y^2), \tag{2}$$

where $\omega_x = q\omega$ and $\omega_y = p\omega$, ω is the common factor of the frequencies by ω_x and ω_y, and p and q are relative prime integers. In terms of action-angle variables $(J_x, J_y, \phi_x, \phi_y)$ and the particle mass m, the representation for the trajectories of Eq. (2) is given by

$$x(t) = \sqrt{\frac{2J_x}{m(q\omega)}}\cos(q\omega t - \phi_x), \tag{3a}$$

$$y(t) = \sqrt{\frac{2J_y}{m(p\omega)}}\cos(p\omega t - \phi_y). \tag{3b}$$

The trajectories for Eq. (3) are the so-called Lissajous figures. Furthermore, four constants of motion for the zero-order system in Eq. (2) are given by [23,24]

$$J = \frac{H_o}{qp\omega} = \frac{1}{qp}(qJ_x + pJ_y), \tag{4a}$$

$$\Delta = \frac{1}{qp}(qJ_x - pJ_y), \tag{4b}$$

$$K = \sqrt{\frac{2J_xJ_y}{qp}}\cos(p\phi_x - q\phi_y), \tag{4c}$$

$$L = \sqrt{\frac{2J_xJ_y}{qp}}\sin(p\phi_x - q\phi_y). \tag{4d}$$

An ensemble of the Lissajous trajectories for a given values of the Cartesian actions (J_x, J_y) is to form a rectangular caus-

 ©2005 The American Physical Society

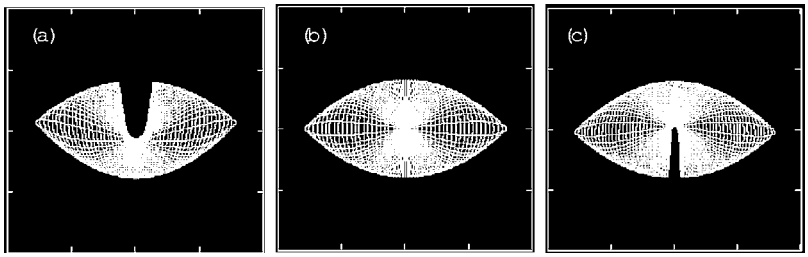

FIG. 1. Family of periodic orbits for the zero-order system with $p:q=2:1$ at a fixed $J=24$ and (a) $K=8$, (b) $K=0$, and (c) $K=-3$.

tic in (x,y) space. Alternatively, J and one of the remaining constants of motion (Δ,K,L) can be used to generate an ensemble of Lissajous trajectories with different shapes of the caustics. Figure 1 depicts the calculated results for a family of trajectories in the zero-order (uncoupled) system with different K values and $J=24$.

To demonstrate the characteristics of the classical trajectories in the coupled system, the coupling potential that is originally considered by Noid *et al.* is employed:

$$V_c = \varepsilon y(x^2 + \eta y^2). \tag{5}$$

Figure 2 displays the numerical results for the typical trajectories of the coupled systems in Eq. (1) for different initial conditions with the parameters of $2\omega_x=\omega_y=2.0$, $\hbar=1$, $\varepsilon=-0.03$, $\eta=-0.2$, and $J=24$. It is clear that the sweeping region of a single trajectory in the coupled system is similar to the caustic formed by an ensemble of the uncoupled system, as shown in Fig. 1. This similarity means that the quantum effect of classical nonlinear resonance can be manifested with the quantum wave functions related to classical periodic orbits in the zero-order systems. As a consequence, the connection between the quantum wave functions and the classical periodic orbits for the zero-order systems can be employed to manifest the quantum features of classical nonlinear resonance [25,26].

III. DERIVATION OF QUANTUM WAVE FUNCTIONS ASSOCIATED WITH CLASSICAL LISSAJOUS TRAJECTORIES

The conventional eigenstates of a 2D harmonic oscillator with commensurate frequencies do not reveal the characteristics of classical Lissajous figures even in the correspondence limit of large quantum number. It is well known that Schrödinger in 1926 [27] originally constructed a coherent state of a one-dimensional (1D) harmonic oscillator to describe a classical particle with a wave packet whose center in the time evolution follows the corresponding classical motion. Extended to 2D system, the Schrödinger coherent state is expected to correspond to a wave packet with its center generally moving along a classical trajectory. This exact correspondence enables us to derive the quantum stationary states localized on the classical Lissajous orbits from the time-dependent Schrödinger coherent state.

Since the Hamiltonian is separable, the Schrödinger coherent state for a 2D harmonic oscillator can be expressed as [27]

$$|\alpha_x,\alpha_y\rangle = \left(\sum_{n_1=0}^{\infty} \frac{|\alpha_x|^{n_1} e^{in_1\phi_x}}{\sqrt{n_1!}} e^{|\alpha_x|^2/2} |n_1\rangle_x e^{-i(n_1+1/2)\omega_x t}\right) \times \left(\sum_{n_2=0}^{\infty} \frac{|\alpha_y|^{n_2} e^{in_2\phi_y}}{\sqrt{n_2!}} e^{|\alpha_y|^2/2} |n_2\rangle_y e^{-i(n_2+1/2)\omega_y t}\right). \tag{6}$$

It can be analytically deduced that the probability density for the coherent state $|\alpha_x,\alpha_y\rangle$ follows the motion of a classical 2D isotropic harmonic oscillator, i.e.,

$$x(t) = \sqrt{\frac{2\hbar}{m\omega_x}}|\alpha_x|\cos(\omega_x t - \phi_x),$$

$$y(t) = \sqrt{\frac{2\hbar}{m\omega_y}}|\alpha_y|\cos(\omega_y t - \phi_y). \tag{7}$$

With this result, the coherent state $|\alpha_x,\alpha_y\rangle$ can be related to the classical trajectory in Eq. (3) by use of the following substitutions:

$$\alpha_x = \sqrt{\frac{J_x}{\hbar}} e^{i\phi_x}, \quad \alpha_y = \sqrt{\frac{J_y}{\hbar}} e^{i\phi_y}. \tag{8}$$

Consider the case of the ratio $\omega_x:\omega_y=q:p$, the set of states with indices (n_1,n_2) in Eq. (6) can be divided into subsets characterized by a pair of indices (u_1,u_2) given by $n_1 \equiv u_1 (\mathrm{mod}\, p)$ and $n_2 \equiv u_2 (\mathrm{mod}\, q)$. In terms of these subsets and the action-angle variables (J_x,J_y,ϕ_x,ϕ_y) in Eq. (8), the Schrödinger coherent state in Eq. (6) can be rewritten as

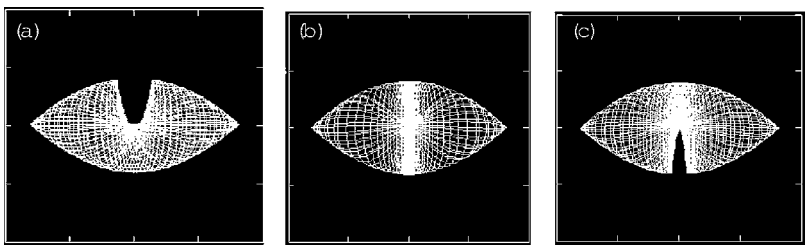

FIG. 2. Classical trajectories for Hamiltonian in Eq. (1) with the coupling potential in Eq. (5) at a fixed $J=24$ and different initial conditions chosen such that the sweeping regions of (a)–(c) similar to the K representation shown in Figs. 1(a)–1(c), respectively.

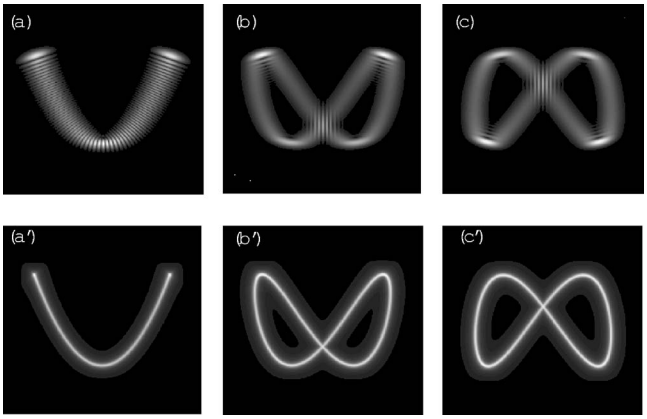

FIG. 3. Comparison between the quantum stationary state $|\Psi_N^{p,q}(x,y;A,\phi)|^2$ [(a)–(c)] and the classical Lissajous orbits [(a)–(c)] for the system of $p:q=2:1$ with $N=40$, $A=5.2$ and (a) $\phi=0$, (b) $\phi=0.3\,\pi$, and (c) $\phi=0.6\,\pi$.

$$|\alpha_x,\alpha_y\rangle = \left(\sum_{u_1=0}^{p-1}\sum_{N_1=0}^{\infty}\frac{(\sqrt{J_x/\hbar})^{pN_1+u_1}e^{i(pN_1+u_1)\phi_x}}{\sqrt{(pN_1+u_1)!}} \times e^{J_x/2\hbar}|pN_1+u_1\rangle_x e^{-i(pN_1+u_1+1/2)q\omega t}\right) \times \left(\sum_{u_2=0}^{q-1}\sum_{N_2=0}^{\infty}\frac{(\sqrt{J_y/\hbar})^{qN_2+u_2}e^{i(qN_2+u_2)\phi_y}}{\sqrt{(qN_2+u_2)!}} \times e^{J_y/2\hbar}|qN_2+u_2\rangle_y e^{-i(qN_2+u_2+1/2)p\omega t}\right). \quad (9)$$

As seen in Eq. (9), the 2D Schrödinger coherent state is divided into a product of two infinite series and two finite series. The method of the triangular partial sums is used to make precise sense out of the product of two infinite series in Eq. (9). Mathematically, the notion of triangular partial sums is called the Cauchy product of the double infinite series [28]. With the representation of the Cauchy product, the terms $|pN_1+u_1\rangle_x|qN_2+u_2\rangle_y$ in Eq. (9) can be arranged diagonally by grouping together those terms for which $N_x+N_y=N$:

$$|\alpha_x,\alpha_y\rangle = \sum_{N=0}^{\infty} e^{(J_x+J_y)/2\hbar}\sum_{u_2=0}^{q-1}\sum_{u_1=0}^{p-1} e^{-i[Npq+(u_1+1/2)q+(u_2+1/2)p]\omega t} \times\left\{\sum_{K=0}^{N}\frac{(\sqrt{J_x/\hbar}e^{i\phi_x})^{pK+u_1}(\sqrt{J_y/\hbar}e^{i\phi_y})^{q(N-K)+u_2}}{\sqrt{(pK+u_1)!}\sqrt{[q(N-K)+u_2]!}} \times|pK+u_1\rangle_x|q(N-K)+u_2\rangle_y\right\}. \quad (10)$$

After some algebra, Eq. (10) can be rewritten as

$$|\alpha_x,\alpha_y\rangle = \sum_{N=0}^{\infty} e^{(J_x+J_y)/2\hbar}\sum_{u_2=0}^{q-1}\sum_{u_1=0}^{p-1} e^{-i[Npq+(u_1+1/2)q+(u_2+1/2)p]\omega t} \times\left(\sqrt{\frac{J_x}{\hbar}}e^{i\phi_x}\right)^{u_1}\left(\sqrt{\frac{J_y}{\hbar}}e^{i\phi_y}\right)^{qN+u_2} \times\left\{\sum_{K=0}^{N}\frac{[\sqrt{(J_x)^p/(J_y)^q}e^{i(p\phi_x-q\phi_y)}]^K}{\sqrt{(pK+u_1)!}\sqrt{[q(N-K)+u_2]!}} \times|pK+u_1\rangle_x|q(N-K)+u_2\rangle_y\right\}. \quad (11)$$

The expression in the curly bracket of Eq. (11) represents the stationary coherent states labeled with one major index N and two minor indices u_1 and u_2. These stationary coherent states are physically expected to be associated with the Lissajous orbits. Since the minor indices u_1 and u_2 essentially do not affect the characteristics of the stationary states, the condition of $u_1=u_2=0$ is used for the following analysis unless otherwise specified. Including the normalization condition, the stationary coherent states in Cartesian coordinates are given by

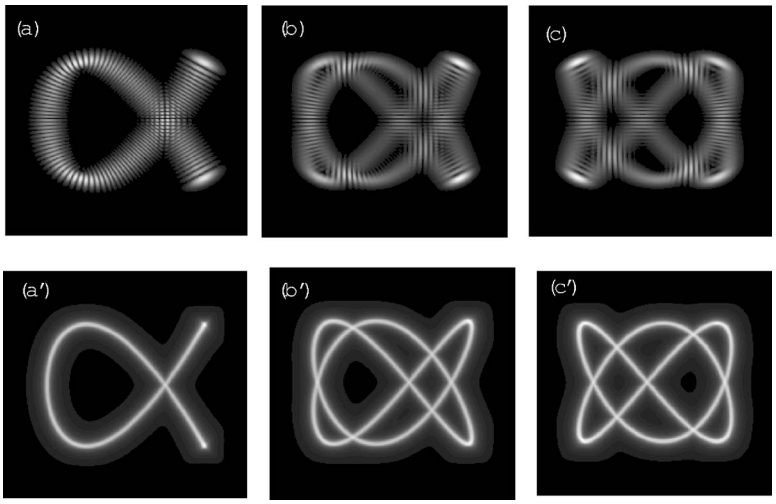

FIG. 4. The same as Fig. 3 for the system of $p:q=3:2$ with $N=22$, $A=5.2$ and (a) $\phi=0$, (b) $\phi=0.3\,\pi$, and (c) $\phi=0.6\,\pi$.

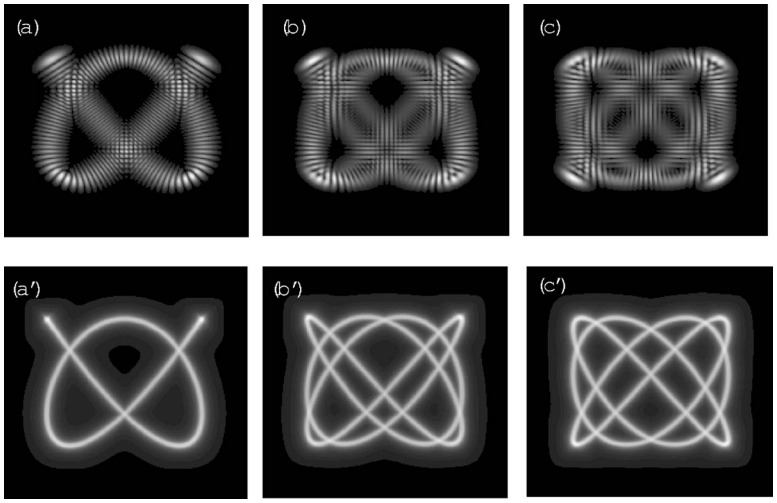

FIG. 5. The same as Fig. 3 for the system of $p:q=4:3$ with $N=15$, $A=5.2$ and (a) $\phi=0$, (b) $\phi=0.3\,\pi$, and (c) $\phi=0.6\,\pi$.

$$\Psi_N^{p,q}(x,y;A,\phi)=\left[\sum_{K=0}^{N}\frac{A^{2K}}{(pK)\,!\,[q(N-K)]!}\right]^{-1/2}\times\sum_{K=0}^{N}\frac{(Ae^{i\phi})^K}{\sqrt{(pK)!\sqrt{[q(N-K)]!}}}\Phi_{pK}(x;\lambda_x)\times\Phi_{q(N-K)}(y;\lambda_y),\tag{12}$$

where

$$A=\sqrt{(J_x)^p/(J_y)^q},\tag{13}$$

$$\phi=p\phi_x-q\phi_y,\tag{14}$$

$$\Phi_n(x;\lambda)=\langle x|n\rangle_x=\sqrt{\frac{\sqrt{\lambda}}{2^n n\,!\,\sqrt{\pi}}}H_n(\sqrt{\lambda}x)e^{-\lambda x^2/2},\tag{15}$$

$H_n(\cdots)$ are the Hermite polynomials, $\lambda_x=m\omega_x/\hbar$, and $\lambda_y=m\omega_y/\hbar$. Equation (12) reveals that the stationary coherent states associated with the Lissajous orbits are the superposition of degenerate eigenstates with the relative amplitude factor A and phase factor ϕ. Equations (13) and (14) indicate that the relative amplitude factor A and phase factor ϕ in the stationary coherent states $\Psi_N^{p,q}(x,y;A,\phi)$ are explicitly related to the classical action-angle variables (J_x,J_y,ϕ_x,ϕ_y).

From Eq. (11), the eigenenergies of the stationary coherent states $\Psi_N^{p,q}(x,y;A,\phi)$ are found to be

$$E_N=\left[Npq+\frac{1}{2}q+\frac{1}{2}p\right]\hbar\omega\underset{N\gg 1}{\rightarrow}(Npq)\hbar\omega.\tag{16}$$

In comparison of Eq. (16) with Eq. (4a), the relationship between the index N and the classical action J is given by

$$J=N\hbar.\tag{17}$$

With Eqs. (12)–(17), the connection between the quantum wave functions and the classical Lissajous orbits is completely manifested. Figures 3–5 depict the comparison between the quantum wave patterns $|\Psi_N^{p,q}(x,y;A,\phi)|^2$ and the corresponding classical periodic orbits for $p:q$ to be 2:1, 3:2, and 4:3, respectively. Here three different phase factors, $\phi=0$, $\phi=0.3\pi$, and $\phi=0.6\pi$, are displayed in each figure for the purpose of clear comparison. The behavior of the quantum wave patterns in all cases can be found to be in precise agreement with the classical Lissajous figures.

It is worthwhile to mention that the stationary states $\Psi_N^{p,q}(x,y;A,\phi)$ for the 2D isotropic harmonic oscillator, i.e., $p:q=1:1$, can be simplified to give rise to the well-known expression of SU(2) elliptic states [29–32]:

$$\Psi_N(x,y;A,\phi)=[1+A^2]^{-N/2}\sum_{K=0}^{N}\frac{\sqrt{N!}}{\sqrt{K!}\sqrt{(N-K)!}}\times(Ae^{i\phi})^K\Phi_K(x;\lambda)\Phi_{N-K}(y;\lambda).\tag{18}$$

In other words, the stationary states $\Psi_N^{p,q}(x,y;A,\phi)$ in Eq. (12) are a kind of SU(2) coherent states. To our knowledge, it is original to derive the stationary coherent states related to the classical Lissajous orbits from the time-dependent Schrödinger coherent state. Since the stationary coherent states $\Psi_N^{p,q}(x,y;A,\phi)$ are well localized on the classical periodic orbits, we call them "localized states."

IV. QUANTUM FEATURES OF CLASSICAL NONLINEAR RESONANCES

As mentioned in Sec. II a classical trajectory in the weakly perturbed systems can be characterized by an ensemble of the unperturbed periodic orbits. The quantum fea-

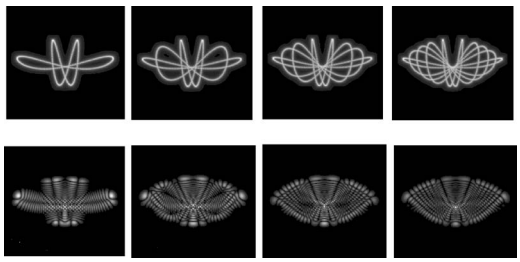

FIG. 6. Calculated results for the variation of the coherent wave patterns (real part) with the number of participant localized states. Top: classical Lissajous trajectories. Bottom: quantum stationary states.

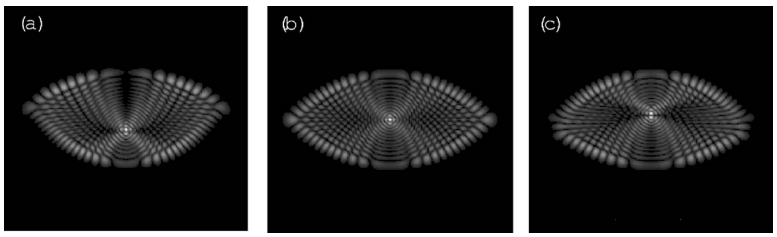

FIG. 7. Quantum wave patterns corresponding to the classical tori shown in Fig. 1.

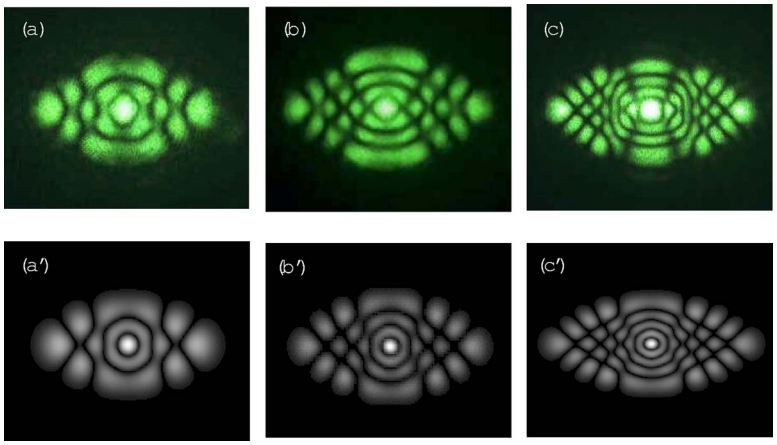

FIG. 8. (Color online) Comparison between the experimental wave patterns [(a)–(c)] observed in the laser experiment and the theoretical patterns of quantum coherent states [(a)–(c)] in a 2:1 intrinsic Fermi resonance.

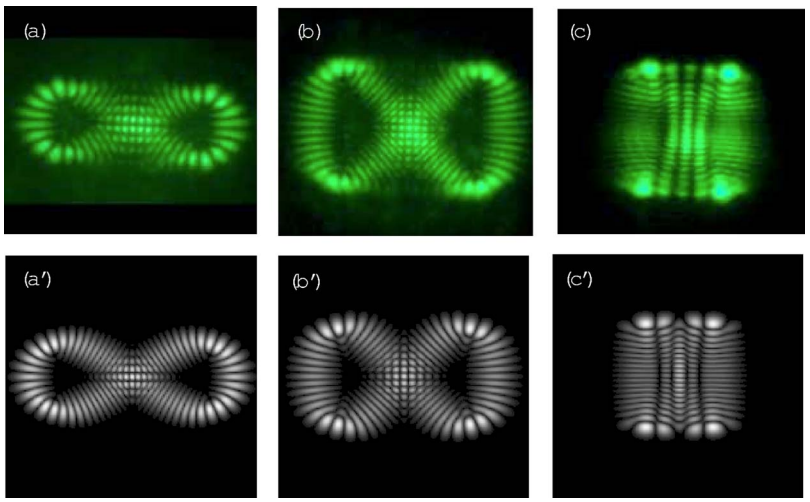

FIG. 9. (Color online) Experimental far-field wave patterns [(a)–(c)] for the stationary figure-eight states that were generated at three different pump positions on the laser crystal, respectively. Theoretical patterns of quantum coherent states $|\Psi_{20}^{2,1}(x,y;A,\pi/2)|^2$ (real part) corresponding to the experimental results: (a) $A=10$, (b) $A=5$, (c) $A=1$.

tures of classical nonlinear resonance can be manifested with a coherent superposition of an ensemble of the localized states. Figure 6 displays the variation of the coherent wave patterns with the number of participant localized states corresponding to the trajectory in Fig. 1(a). It is found that only a few localized states are already sufficient to form a well extended pattern within the classical caustics, similar to a kaleidoscopic pattern. The high efficiency of the wave extension comes from the fact that the encompassing region of each localized state covers a width of several de Broglie wavelengths. Since the de Broglie wavelength is inversely proportional to $\sqrt{N}$, the critical number of localized states for a well extended pattern is of order $\sqrt{N}$. In other words, the highly efficient extension of the wave pattern is a salient quantum phenomenon in mesoscopic systems with nonlinear resonances. Figure 7 depicts the quantum wave functions corresponding to the classical tori shown in Fig. 1. A close classical quantum correspondence can be clearly seen; the quantum wave distributions are well extended within the associated classical caustics. In the following section, we give an intriguing demonstration that the laser cavity is a promising analogous experiment for visualizing the quantum wave functions associated with nonlinear resonances.

V. ANALOGOUS EXPERIMENTAL OBSERVATIONS

In recent years, microwave cavities have been used to perform analog studies of transport in open quantum dots [33–35]. Recently, Doya *et al.* [36] have introduced the paraxial approximation to establish an analogy between light propagation along a multimode fiber and quantum confined systems. Furthermore, we have demonstrated that it is promising to explore the high-order quantum wave function from the pattern formation of the laser resonators [37–39]. This demonstration is based on the fact that the wave equation for the transverse mode of the laser resonators in the paraxial approximation is in analogy with the Schrödinger equation for the 2D quantum confined systems [40,41]. More recently, we have observed the kaleidoscope of laser patterns in a near-hemispheric microchip laser with an intracavity saturable absorber [42]. However, the origin of the salient pattern formation was not clearly understood at that moment. Here we demonstrate that the observed laser modes are a kind of analogous wave patterns associated with the quantum coherent states in a 2:1 stretch-bend Fermi resonance.

The experimental configuration in Ref. [42] is a near-hemispheric cavity in which the transverse mode spacing $\Delta\nu_T$ and the longitudinal mode spacing $\Delta\nu_L$ are very close to be commensurable, i.e., $\Delta\nu_L:\Delta\nu_T \approx 2:1$. The inherent commensurability between $\Delta\nu_T$ and $\Delta\nu_L$ have a dramatic effect on the formation of laser patterns, as shown in the internal nonlinear resonances. In other words, the coupling of a 2:1 longitudinal-transverse resonance is identical in form to the well-known phenomenon of Fermi resonance in molecular systems. We have redone the experiment but with a semiconductor quantum well instead of a bulk crystal as a saturable absorber in the laser cavity. Similar patterns to those found in Ref. [42] can be almost reproduced. This similarity implies that the observed patterns are insensitive to the types of the saturable absorbers, even though the saturable absorber provides a source of nonlinear coupling. As shown in Fig. 8, the formation of the observed laser patterns can be well explained with the quantum coherent states of a 2:1 intrinsic Fermi resonance. Note that the bright spot near the center of the kaleidoscopic patterns arises from the quantum-classical correspondence that all figure-eight classical orbits pass through the focal point near origin. The excellent agreement between the experimental and theoretical patterns confirms that the coupling of a 2:1 longitudinal-transverse resonance in a near-hemispheric laser resonator is analogous to the well-known phenomenon of Fermi resonance in molecular systems. The present analysis also provides a further indication that laser resonators can be designed to demonstrate the quantum phenomenon in mesoscopic physics [43].

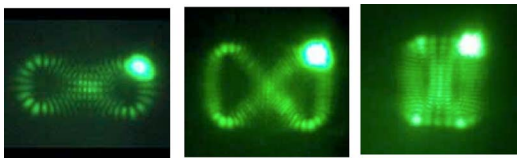

FIG. 10. (Color online) Experimental images of the wave intensities on the laser crystal corresponding to the experimental far-field patterns shown in Fig. 9, respectively. The bright spot on the experimental image represents the location of the pump beam.

With the same laser cavity configuration, the stationary localized states related to the single figure-eight classical orbits can be excited by use of the off-axis pumping scheme. Figure 9 shows three experimental far-field patterns for the stationary figure-eight states that were generated at different off-axis pump positions on the laser crystal, respectively. The theoretical patterns corresponding to the experimental results are also plotted in Fig. 9 for comparison. Again, excellent agreement is found for all cases. Figure 10 shows the experimental images of the field intensities on the laser crystal to reveal the relationship between the pump positions and the formation of the stationary localized states. The bright spot on the experimental image in Fig. 10 represents the location of the pump beam. It can be seen that the formation of the stationary figure-eight states is primarily dependent on the overlap between the pump intensity and the lasing mode distribution. This is consistent with the fact that the cavity mode with the biggest overlap with the gain region will dominate the lasing process. As a consequence, controlling the pump position can straightforwardly manipulate the generation of different stationary localized figure-eight states in a near-hemispheric resonator. Nowadays, manipulation of the spatially localized optical wave may be promising for optical information process applications [44]. One central part of the theory in Sec. III is to derive the analytical representation for the stationary Lissajous states. Our experimental results illustrate that this analytical representation is not only important for understanding the quantum features of the mesoscopic states with nonlinear coupling but also useful for providing the idea to manipulate the generation of the stationary localized states in laser cavities. For the first time to our knowledge, the analytic representation for the stationary Lissajous states is derived and employed to explore the manipulation properties of the coherent optical wave in a degenerate laser cavity.

VI. CONCLUSIONS

In summary, we have analytically derived the stationary coherent states associated with the classical Lissajous orbits from the Schrödinger coherent states for the 2D harmonic oscillators with commensurate frequencies. We have employed the connection between the quantum wave functions and the classical Lissajous orbits for the zero-order systems to investigate the quantum features of classical nonlinear resonances. It is found that the highly efficient extension of the quantum wave functions within the classical caustics is an intriguing phenomenon in mesoscopic systems with nonlinear coupling resonances. Furthermore, we have theoretically and experimentally demonstrated that a nearly hemispherical laser resonator with an intracavity saturable absorber forms an experimental system for visualizing the quantum wave functions associated with Fermi resonance.

ACKNOWLEDGMENT

The author thanks the National Science Council for their financial support of this research under Contract No. NSC-94-2112-M-009-034.

[1] J. P. Bird, R. Akis, D. K. Ferry, A. P. S. de Moura, Y. C. Lai, and K. M. Indlekofer, Rep. Prog. Phys. **66**, 583 (2003).
[2] I. V. Zozoulenko and K. F. Berggren, Phys. Rev. B **56**, 6931 (1997).
[3] Y. Takagaki and K. H. Ploog, Phys. Rev. E **62**, 4804 (2000).
[4] D. K. Ferry, R. Akis, and J. P. Bird, J. Phys.: Condens. Matter **17**, S1017 (2005).
[5] L. Christensson, H. Linke, P. Ornling, P. E. Lindelof, I. V. Zozoulenko, and K. F. Berggren, Phys. Rev. B **57**, 12306 (1998).
[6] Y. H. Kim, M. Barth, U. Kuhl, H. J. Stöckmann, and J. P. Bird, Phys. Rev. B **68**, 045315 (2003).
[7] W. Li, L. E. Reichl, and B. Wu, Phys. Rev. E **65**, 056220 (2002).
[8] R. Narevich, R. E. Prange, and O. Zaitsev, Phys. Rev. E **62**, 2046 (2000).
[9] J. Wiersig, Phys. Rev. E **64**, 026212 (2001).
[10] J. A. de Sales and J. Florencio, Physica A **290**, 101 (2001).
[11] M. Brack and R. K. Bhaduri, *Semiclassical Physics* (Addison-Wesley, Reading, MA, 1997), Sec. 2.7.
[12] F. von Oppen, Phys. Rev. B **50**, 17151 (1994).
[13] R. W. Robinett, Am. J. Phys. **65**, 1167 (1997).
[14] Y. F. Chen, K. F. Huang, and Y. P. Lan, Phys. Rev. E **66**, 046215 (2002).
[15] Y. F. Chen, K. F. Huang, and Y. P. Lan, Phys. Rev. E **66**, 066210 (2002).
[16] Y. F. Chen and K. F. Huang, Phys. Rev. E **68**, 066207 (2003).
[17] Y. F. Chen and K. F. Huang, J. Phys. A **36**, 7751 (2003).
[18] E. Fermi, Z. Phys. **71**, 250 (1931).
[19] D. W. Noid, M. L. Koszykowski, and R. A. Marcus, J. Chem. Phys. **71**, 2864 (1979).
[20] D. Farrelly and T. Uzer, J. Chem. Phys. **84**, 308 (1986).
[21] G. Contopoulos and B. Barbanis, Astron. Astrophys. **153**, 44 (1985).
[22] A. Elipe, Phys. Rev. E **61**, 6477 (2000).
[23] H. Goldstein, *Classical Mechanics* (Addison-Wesley, Reading, MA, 1980).
[24] C. C. Martens and G. S. Ezra, J. Chem. Phys. **87**, 284 (1987).
[25] M. C. Gutzwiller, *Chaos in Classical and Quantum Mechanics* (Springer-Verlag, New York, 1990).
[26] M. V. Berry and M. Tabor, Proc. R. Soc. London, Ser. A **349**, 101 (1976).
[27] E. Schrödinger, Naturwiss. **14**, 644 (1926).
[28] G. B. Folland, *Advanced Calculus* (Prentice-Hall, Upper Saddle River, NJ, 2002).
[29] V. Bužek and T. Quang, J. Opt. Soc. Am. B **6**, 2447 (1989).
[30] S. De Bièvre, J. Phys. A **25**, 3399 (1992).
[31] J. Pollet, O. Méplan, and C. Gignoux, J. Phys. A **28**, 7287 (1995).
[32] J. Banerji and G. S. Agarwal, Opt. Express **5**, 220 (1999).
[33] Y. H. Kim, M. Barth, H. J. Stöckmann, and J. P. Bird, Phys. Rev. B **65**, 165317 (2002).
[34] R. G. Nazmitdinov, K. N. Pichugin, I. Rotter, and P. Šeba, Phys. Rev. B **66**, 085322 (2002).
[35] T. Blomquist, H. Schanze, I. V. Zozoulenko, and H. J. Stöckmann, Phys. Rev. E **66**, 026217 (2002).
[36] V. Doya, O. Legrand, F. Mortessagne, and C. Miniatura, Phys. Rev. Lett. **88**, 014102 (2002).
[37] K. F. Huang, Y. F. Chen, H. C. Lai, and Y. P. Lan, Phys. Rev. Lett. **89**, 224102 (2002).
[38] Y. F. Chen and Y. P. Lan, Phys. Rev. A **66**, 053812 (2002).
[39] Y. F. Chen, K. F. Huang, H. C. Lai, and Y. P. Lan, Phys. Rev. E **68**, 026210 (2003).
[40] S. Danakas and P. K. Aravind, Phys. Rev. A **45**, 1973 (1992).
[41] A. E. Siegman, *Lasers* (University Science Books, Mill Valley, CA, 1986).
[42] Y. F. Chen and Y. P. Lan, Phys. Rev. Lett. **93**, 013901 (2004).
[43] D. Dragoman and M. Dragoman, Prog. Quantum Electron. **23**, 131 (1999).
[44] K. Staliunas, *Transverse Patterns in Nonlinear Optical Resonators*, Springer Tracts in Modern Physics Vol. 183 (Springer, Berlin, 2003), p. 1.